Inorganic Chemistry

Article

pubs.acs.org/IC

Pentanuclear Heterometallic $\{Mn^{III}_2Ln_3\}$ (Ln = Gd, Dy, Tb, Ho) Assemblies in an Open-Book Type Structural Topology: Appearance of Slow Relaxation of Magnetization in the Dy(III) and Ho(III) Analogues

Prasenjit Bag,[†] Amit Chakraborty,[†] Guillaume Rogez,*[,‡] and Vadapalli Chandrasekhar*[,†,§]

[†]Department of Chemistry, Indian Institute of Technology Kanpur, Kanpur 208016, India

[‡]Institut de Physique et Chimie des Matériaux de Strasbourg, UMR 7504 CNRS-Université de Strasbourg, 23 rue du Loess, B.P. 43, 67034 Strasbourg Cedex 2, France

[§]National Institute of Science Education and Research, Institute of Physics Campus, Sachivalaya Marg, Sainik School Road, Bhubaneshwar 751 005, Odisha, India

Supporting Information

ABSTRACT: The reaction of Ln(III) nitrate and $Mn(ClO_4)_2\cdot 6H_2O$ salts in the presence of a multidentate sterically unencumbered ligand, (*E*)-2,2′-(2-hydroxy-3-((2-hydroxyphenylimino)methyl)-5-methylbenzylazanediyl)-diethanol ($\mathbf{LH_4}$) leads to the isolation of four isostructural pentanuclear hetereometallic complexes $[Mn^{III}_2Gd_3(LH)_4(NO_3)(HOCH_3)]ClO_4\cdot NO_3$ (**1**), $[Mn^{III}_2Dy_3(LH)_4(NO_3)(HOCH_3)]ClO_4\cdot NO_3$ (**2**), $[Mn^{III}_2Tb_3(LH)_4(NO_3)(HOCH_3)]ClO_4\cdot NO_3$ (**3**), and $[Mn^{III}_2Ho_3(LH)_4(NO_3)(HOCH_3)]ClO_4\cdot NO_3$ (**4**) with an open-book type structural topology. **1**−**4** are dicationic and crystallize in the achiral space group, $P2_1/n$. A total of four triply deprotonated ligands, $[LH]^{3-}$, are involved in holding the pentameric metal framework, $\{Mn^{III}_2Ln_3\}$. In these complexes both the lanthanide and the manganese(III) ions are doubly bridged, involving phenolate or ethoxide oxygen atoms. The magnetochemical analysis reveals the presence of global antiferromagnetic interactions among the spin centers at low temperatures in all the four compounds. AC susceptibility measurements show the presence of temperature dependent out-of-phase *ac* signal for compounds **2** and **4** indicating an SMM behavior.

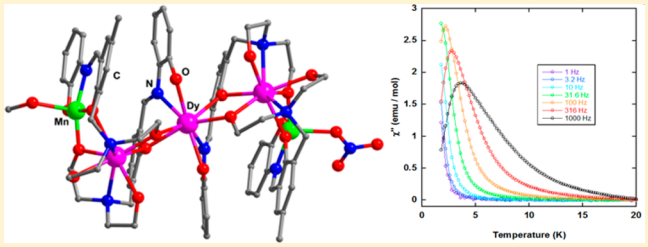

INTRODUCTION

The discovery of the single molecule magnet (SMM) behavior in $[Mn_{12}O_{12}(O_2CR)_{16}(H_2O)_4]$ (R = Me, Ph)[1] gave birth to a new field of activity in molecular materials.[2] Although molecular magnetism was already under intense investigation, the realization that even at the molecular level, phenomena that are typically associated with bulk behavior, such as permanent magnet behavior,[3] can be observed, resulted in a major paradigm change in this interdisciplinary field. Chemists, physicists, and materials scientists were equally interested in the new phenomena, each with a different perspective. While the physicists viewed these new objects with interest because of the opportunity they presented to address questions related to quantum objects,[4] for the materials scientists, SMMs[5] represented a new generation of materials with a lot of potential applications in data storage,[6] quantum computation,[7] magnetic refrigeration,[8] and so forth. From the perspective of the synthetic chemists, SMMs and related compounds represented a challenge in terms of design, assembly, and structure−property correlation. Thus, the chemists had the challenge, through synthesis, to control the two most important ingredients that seem to be responsible for SMM behavior, viz., a high ground-state spin (S) and a significant uniaxial magnetic anisotropy (D).[9] With these features in mind, several types of compounds have been investigated: polynuclear homometallic 3d complexes,[10] 4f complexes,[11] and mixed metal 3d/4f complexes.[12] The latter, in particular, have been attracting considerable interest. Among the 3d/4f complexes, although the initial studies focused on Cu^{II}/Ln^{III} complexes,[13] recently there has been a shift toward Mn^{III}/Ln^{III} complexes.[14] This is because manganese(III) complexes, apart from high spin, because of Jahn−Teller distortion possess significant magnetic anisotropy. However, the main challenge involves designing appropriate ligands that can deliver complexes possessing precise placement of the diverse metal ions such that the optimal magnetic properties can be extracted. A survey of the literature reveals that many high nuclearity Mn^{III}/Ln^{III} clusters are well-known.[14a−h] In contrast, low nuclearity analogues are still quite sparse.[15] A notable advantage of the latter is that they

Received: November 20, 2013
Published: June 6, 2014

   dx.doi.org/10.1021/ic4028833 | *Inorg. Chem.* 2014, 53, 6524−6533

Scheme 1. Synthesis of Complexes 1−4[a]

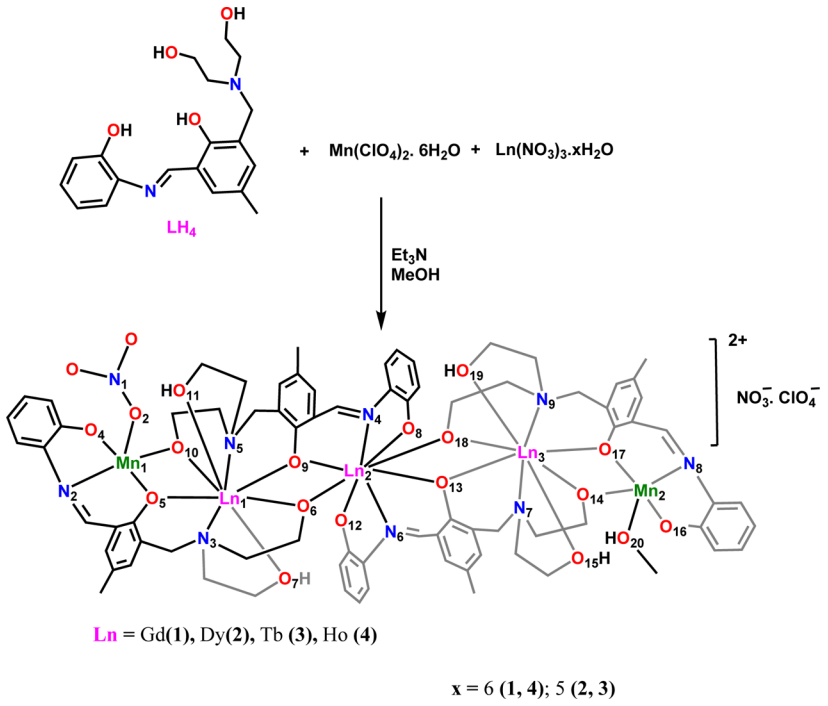

[a]Atom numbering applicable to compound **2**.

allow easier understanding of the magnetic behavior. With this reasoning we have recently prepared tetranuclear Mn^{III}_2/Ln^{III}_2 compounds that possessed an arch-type topology; some members of this family showed SMM behavior.[16] Spurred by this, we have designed a multidentate sterically unemcumbered flexible ligand, (*E*)-2,2′-(2-hydroxy-3-((2-hydroxyphenylimino)methyl)-5-methylbenzylazanediyl)-diethanol (LH_4) which was used recently to prepare a $Ni^{II}_2Ln^{III}_3$ family.[17] Utilizing this ligand we now have been successful in isolating four dicationic pentanuclear heterometallic $\{Mn^{III}_2Ln^{III}_3\}$ [Ln(III) = Gd (**1**), Dy (**2**), Tb (**3**), Ho (**4**)] complexes whose metallic cores possess an open-book type structural topology (similar to one of the conformations of H_2O_2). Magnetic studies on these complexes reveal the presence of SMM behavior in the Dy^{III} and Ho^{III} analogues. These are discussed herein.

EXPERIMENTAL SECTION

Reagents and General Procedures. Solvents and other general reagents used in this work were purified according to standard procedures.[18] Anhydrous magnesium chloride (Alfa Aesar, Hyderabad, India) was used as purchased. Diethanolamine, *p*-cresol, paraformaldehyde, and 2-aminophenol were obtained from SD. Fine Chemicals, Mumbai, India and were used as received. $Mn(ClO_4)_2{\cdot}6H_2O$, $Ln(NO_3)_3{\cdot}xH_2O$ were obtained from Aldrich Chemical Co. USA and were used without any further purification. (*E*)-2,2′-(2-Hydroxy-3-((2-hydroxyphenylimino)methyl)-5-methylbenzylazanediyl)diethanol (LH_4) was synthesized according to a literature procedure.[17]

Synthesis. *Preparation of the Tetranuclear Complexes 1−4.* A general protocol was employed for the preparation of all the metal complexes (**1**−**4**) as follows. LH_4 (0.074 g, 0.20 mmol) was dissolved in methanol (10 mL). $Ln(NO_3)_3{\cdot}xH_2O$ (0.20 mmol) and triethylamine (0.50 mmol) were added to this solution. The reaction mixture was stirred for 30 min. At this stage, $Mn(ClO_4)_2{\cdot}6H_2O$ (0.040 g, 0.11 mmol) was added, and the reaction mixture was stirred for a further period of 3 h at room temperature to afford a clear deep brown solution. Then, the solution was filtered and kept in a vial for crystallization at room temperature. Dark red-brown block-shaped crystals appeared in 4−5 days. The characterization data for these complexes are given below.

*$[Mn_2Gd_3(LH)_4(NO_3)(HOCH_3)]ClO_4{\cdot}NO_3{\cdot}5CH_3OH{\cdot}H_2O$ (**1**).* Yield: 0.056 g (35.4% based on Gd). Mp: >250 °C. IR (KBr), cm^{-1}: 3428 (b), 2973 (w), 2917 (m), 2847(s), 1599 (s), 1582 (s) 1557 (s) 1476 (s), 1383 (s), 1303 (s), 1280 (m), 1185 (s), 1148 (s), 1079 (s). ESI-MS *m*/*z*, ion: 1032.64 $[M + Na + H^-]^{2+}$. Anal. Calcd for $C_{82}H_{110}N_{10}O_{33}ClMn_2Gd_3$ (2380.88 g mol^{-1}): C, 41.37; H, 4.66; N, 5.88%. Found: C, 40.85; H, 4.34; N, 5.67%.

*$[Mn_2Dy_3(LH)_4(NO_3)(HOCH_3)]ClO_4{\cdot}NO_3{\cdot}4CH_3OH{\cdot}H_2O$ (**2**).* Yield: 0.066 g (41.7% based on Dy). Mp: >250 °C. IR (KBr), cm^{-1}: 3430 (b), 2974 (w), 2916 (m), 2849 (s), 1599 (s), 1582 (s) 1557 (s) 1476 (s), 1383 (s), 1304 (s), 1281 (m), 1185 (s), 1149 (s), 1081 (s). ESI-MS *m*/*z*, ion: 1040.65, $[M + Na + H^-]^{2+}$. Anal. Calcd for $C_{58}H_{96}N_6O_{32}Mn_2Gd_2$ (2364.59 g mol^{-1}): C, 41.14; H, 4.52; N, 5.92%. Found: C, 40.61; H, 4.18; N, 5.69%.

*$[Mn_2Tb_3(LH)_4(NO_3)(HOCH_3)]ClO_4{\cdot}NO_3{\cdot}3CH_3OH{\cdot}H_2O$ (**3**).* Yield: 0.070 g (44.8% based on Tb). Mp: >250 °C. IR (KBr), cm^{-1}: 3427 (b), 2975 (w), 2915 (m), 2849 (s), 1599 (s), 1582 (s) 1557 (s) 1476 (s), 1383 (s), 1304 (s), 1281 (m), 1185 (s), 1149 (s), 1080 (s). ESI-MS *m*/*z*, ion: 1034.65, $[M + Na + H^-]^{2+}$. Anal. Calcd for $C_{80}H_{102}N_{10}O_{31}ClMn_2Tb_3$ (2321.81 g mol^{-1}): C, 41.38; H, 4.43; N, 6.03%. Found: C, 40.81; H, 4.07; N, 5.78%.

*$[Mn_2Ho_3(LH)_4(NO_3)(HOCH_3)]ClO_4{\cdot}NO_3{\cdot}3CH_3OH{\cdot}H_2O$ (**4**).* Yield: 0.050 g (32.1% based on Ho). Mp: >250 °C. IR (KBr), cm^{-1}: 3425 (b), 2976 (w), 2916 (m), 2850 (s), 1599 (s), 1582 (s) 1557 (s) 1476 (s), 1383 (s), 1304 (s), 1281 (m), 1185 (s), 1149 (s), 1081 (s). ESI-MS *m*/*z*, ion: 1043.65, $[M + Na + H^-]^{2+}$. Anal. Calcd for $C_{80}H_{102}N_{10}O_{31}ClMn_2Ho_3$ (2339.84 g mol^{-1}): C, 41.07; H, 4.39; N, 5.99%. Found: C, 40.53; H, 4.03; N, 5.79%.

Instrumentation. Melting points were measured using a JSGW melting point apparatus and are uncorrected. IR spectra were recorded as KBr pellets on a Bruker Vector 22 FT-IR spectrophotometer operating at 400−4000 cm^{-1}. ^1H NMR was recorded on a JEOL-JNM LAMBDA model 400 spectrometer using CD_3OD operating at 400 MHz. Elemental analyses of the compounds were obtained from Thermoquest CE instruments CHNS-O, EA/110 model. Electrospray ionization mass spectrometry (ESI-MS) spectra were recorded on a

dx.doi.org/10.1021/ic4028833 | *Inorg. Chem.* 2014, 53, 6524−6533

Table 1. Details of the Data Collection and Refinement Parameters for Compounds 1−4

	1	2	3	4
Formula	$C_{82}H_{110}N_{10}O_{33}$ Cl Mn_2Gd_3	$C_{82}H_{110}N_{10}O_{33}$ Cl Mn_2Dy_3	$C_{80}H_{102}$ $N_{10}O_{31}Cl$ Mn_2Tb_3	$C_{80}H_{102}$ $N_{10}O_{31}Cl$ Mn_2Ho_3
M/g	2380.88	2396.64	2321.81	2339.84
crystal system	Monoclinic	Monoclinic	Monoclinic	Monoclinic
space group	$P2_1/n$	$P2_1/n$	$P2_1/n$	$P2_1/n$
wavelength (Mo Kα)	0.710 73	0.710 73	0.710 73	0.710 73
unit cell dimensions (Å, deg)	a = 14.6947(9)	a = 14.6979(14)	a = 14.6942(17)	a = 14.657(5)
	b = 37.198(2)	b = 37.163(3)	b = 37.104(4)	b = 37.027(5)
	c = 16.7241(11)	c = 16.6855(15)	c = 16.773(2)	c = 16.650(5)
	α = 90	α = 90	α = 90	α = 90.000(5)
	β = 90.030(2)	β = 90.240(2)	β = 90.235(3)	β = 90.307(5)
	γ = 90	γ = 90	γ = 90	γ = 90.000(5)
V/Å^3	9141.6(10)	9113.9(14)	9145.0(19)	9036(4)
Z	4	4	4	4
ρ_c/g cm^{-3}	1.730	1.747	1.686	1.720
μ/mm^{-1}	2.533	2.818	2.673	2.984
F(000)	4780	4804	4648	4672
cryst size (mm^3)	0.14 × 0.115 × 0.095	0.12 × 0.105 × 0.085	0.135 × 0.11 × 0.09	0.125 × 0.105 × 0.09
θ range (deg)	2.14 to 26.00	2.05 to 26.00	1.10 to 27.00	1.10 to 26.00
limiting indices	$-18 \le h \le 18$,	$-18 \le h \le 12$,	$-18 \le h \le 18$,	$-17 \le h \le 18$,
	$-45 \le k \le 45$,	$-45 \le k \le 45$,	$-47 \le k \le 47$,	$-45 \le k \le 39$,
	$-20 \le l \le 15$	$-20 \le l \le 20$	$-21 \le l \le 21$	$-20 \le l \le 18$
reflns collected	69 189	66 525	153 293	50 868
ind reflns	17 963	17 848	19 967	17 663
	[R(int) = 0.0699]	[R(int) = 0.0921]	[R(int) = 0.0544]	[R(int) = 0.0918]
completeness to θ (%)	99.9	99.0	100.0	99.4
refinement method	Full-matrix-block least-squares on F^2	Full-matrix-block least-squares on F^2	Full-matrix-block least-squares on F^2	Full-matrix-block least-squares on F^2
data/restraints/params	17963/34/1213	15954/54/1213	19967/53/1167	17663/46/1173
goodness-of-fit on F^2	1.036	1.032	1.151	1.037
final R indices [$I > 2\theta(I)$]	$R1$ = 0.0451,	$R1$ = 0.0417,	$R1$ = 0.0509,	$R1$ = 0.0629,
	$wR2$ = 0.0952	$wR2$ = 0.0903	$wR2$ = 0.1235	$wR2$ = 0.1494
R indices (all data)	$R1$ = 0.0713,	$R1$ = 0.0646,	$R1$ = 0.0601,	$R1$ = 0.1126,
	$wR2$ = 0.1043	$wR2$ = 0.0978	$wR2$ = 0.1287	$wR2$ = 0.1869
largest diff. peak and hole (e·Å^{-3})	1.539 and −1.264	2.430 and −1.229	2.629 and −1.389	2.453 and −1.330

Micromass Quattro II triple quadrupole mass spectrometer. Electrospray ionization (positive ion, full scan mode) was used employing methanol as the solvent for desolvation. Capillary voltage was maintained at 2 kV, and the cone voltage was kept at 31 kV. Magnetic measurements were performed using a Quantum Design SQUID-VSM magnetometer. The samples were blocked in eicosane to prevent orientation under magnetic field. Magnetization measurements at different fields at a given temperature confirm the absence of ferromagnetic impurities. Data were corrected for the sample holder and diamagnetism was estimated from Pascal constants.

X-ray Crystallography. The crystal data and the cell parameters for **1**−**4** are given in Table 1. The crystal data for **1**−**4** have been collected on a Bruker SMART CCD diffractometer using a Mo Kα sealed tube. The program *SMART*[19a] was used for collecting frames of data, indexing reflections, and determining lattice parameters, *SAINT*[19a] for integration of the intensity of reflections and scaling, *SADABS*[19b] for absorption correction, and *SHELXTL*[19c,d] for space group and structure determination and least-squares refinements on F^2. All the structures were solved by direct methods using the programs *SHELXS-97*[19e] and refined by full-matrix least-squares methods against F^2 with *SHELXL-97*.[19e] Hydrogen atoms were fixed at calculated positions, and their positions were refined by a riding model. All the non-hydrogen atoms were refined with anisotropic displacement parameters. The crystallographic figures used in this manuscript have been generated using *Diamond 3.1e* software.[19f]

In all the crystals the presence of short inter D-H..H-X contacts in the 'A' alert (CIF in Supporting Information) can be attributed to the crystal packing and moderately high thermal parameters of some solvent MeOH molecules. This compels H atoms to come close to each other.

RESULTS AND DISCUSSION

Synthetic Aspects. The synthesis of LH_4 involved the Schiff-base condensation reaction of 3-((bis(2-hydroxyethyl)-amino)methyl)-2-hydroxy-5-methylbenzaldehyde with 2-aminophenol in methanol and has been reported by us previously.[17] The interesting feature of this ligand is that it is composed of two coordination compartments; one side is composed of the chelating ONO donor platform and the other side consists of a phenolic oxygen and a flexible diethanolamine group (tetradentate OONO donor site). Thus, LH_4 has effectively 6 potential coordination sites with a potential to assemble multinuclear compounds. Also, another important aspect that can be envisaged from our previous experience[16,17] is that while the *free form* of the ethanolamine oxygen ($-CH_2OH$) can function as a terminal ligand, its deprotonated form ($-CH_2O$) can play a pivotal role in expanding the cluster size through its bridging coordination action.[20] In this context it may be mentioned that, employing the same ligand (LH_4),

dx.doi.org/10.1021/ic4028833 | Inorg. Chem. 2014, 53, 6524−6533

recently we reported four Ni_2Ln_3 complexes (Ln = Dy, Gd, Tb, Ho), among which dysprosium derivative showed a multistep relaxation. We also observed a hysteresis loop below 3 K.[17] In view of this background we were interested in extending these studies to the analogous Mn(III) derivatives. Accordingly, the reaction of LH_4, $Mn(ClO_4)_2{\cdot}6H_2O$, and $Ln(NO_3)_3{\cdot}6H_2O$ in the presence of triethylamine as the base afforded the heterometallic pentanuclear monocationic complex salts $[Mn^{III}_2Ln_3(LH)_4(NO_3)(MeOH)]ClO_4{\cdot}NO_3$ (**1**–**4**) in excellent yields (Scheme 2, eq 1; see also Experimental Section). In complexes **1**–**4**, manganese is present in an oxidation state of +3; aerial oxidation in basic medium seems to be the process oxidizing Mn(II) to Mn(III).[14b,16] The molecular structures of all the complexes were determined by single-crystal X-ray crystallography (vide infra). The stability of all the compounds in solution could be established by the detection of their prominent molecular ion peaks $[M^{2+} + Na^+ + H^-]^{2+}$, under ESI-MS condition (see Experimental Section, Supporting Information). It is interesting to note that there is only one previous instance of Mn_2Ln_3 complexes that are known. These were prepared using *N*-butyldiethanolamine and pivalic acid ligands and contain an alternate placement of the lanthanide ions in an overall semicircular architecture (Figure 1).[21]

$$2Mn(ClO_4)_2 + 3Ln(NO_3)_3 + 4LH_4 + 10Et_3N + 0.5O_2 \rightarrow [Mn^{III}_2Ln_3(LH)_4(NO_3)(CH_3OH)](ClO_4){\cdot}(NO_3) + 3Et_3NH\,ClO_4 + 7Et_3NH\,NO_3 + H_2O \quad (1)$$

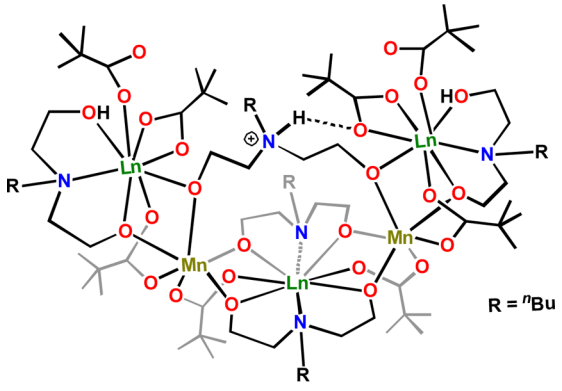

Ln= Y, Tb, Dy, Ho, Er

Figure 1. Previously known Mn_2(III)Ln_3 family.[22]

X-ray Crystallography. X-ray quality crystals of **1**–**4** were obtained over a week by slow evaporation from the methanolic solution of the corresponding complexes. Single crystal X-ray analysis revealed that all four compounds are dicationic and crystallize in the monoclinic space group $P2_1/n$. The asymmetric unit of all the compounds comprises a full molecule, viz., $[Mn^{III}_2Ln_3\,(LH)_4]NO_3{\cdot}ClO_4$.

All the compounds (**1**–**4**) are isomorphous and dicationic. The two manganese ions are present at the two ends of the complex and are separated by an almost linear trinuclear lanthanide $\{Ln_3\}$ unit. In this regard they are different from the previously known analogues (Figure 1). The charge in **1**–**4** is balanced by one perchlorate and one nitrate counteranion. In view of the isostructural nature of these complexes we have chosen $[Mn^{III}_2Dy_3(LH)_4]^{2+}$ (**2**) as a representative example to describe the overall molecular structure. The structural features of this compound are detailed in Figures 2–7. Selected bond

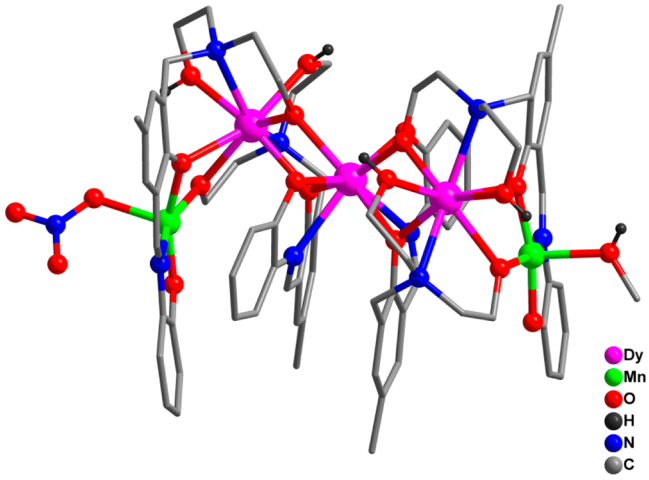

Figure 2. Molecular structure of **2** (hydrogen atoms, counteranions, and solvent molecules were omitted for clarity).

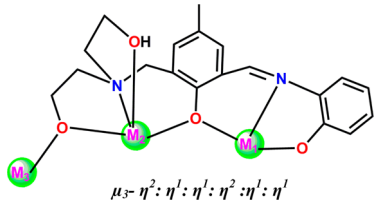

Figure 3. Binding mode of the ligand ($[LH]^{3-}$) with the metal ions.

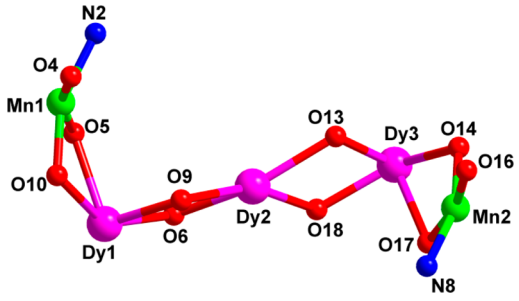

Figure 4. View of the of central Mn_2Dy_3 core in **2** the arrangement of the two planes, each of them constitute with {Dy3} unit and one of the Mn(III) ion. Selected bond distances (Å) and bond angles (deg) are as follows: Mn(1)–O(4) = 1.862(4), Mn(1)–O(10) = 1.875(4), Mn(1)–O(5) = 1.909(4), Mn(1)–N(2) = 1.989(5), Mn(2)–O(16) = 1.857(4), Mn(2)–O(14) = 1.875(4), Mn(2)–O(17) = 1.910(4), Mn(2)–N(8) = 1.986(5), Dy(1)–O(10) = 2.348(4), Dy(1)–O(5) = 2.442(4), Dy(1)–O(6) = 2.244(4), Dy(1)–O(9) = 2.310(4), Dy(2)–O(6) = 2.306(4), Dy(2)–O(9) = 2.421(4), Dy(3)–O(18) = 2.238(4), Dy(3)–O(13) = 2.279(4), Dy(3)–O(18) = 2.238(4), Dy(3)–O(13) = 2.279(4), Dy(3)–O(19) = 2.401(4), Dy(1)–Mn(1) = 3.3970(10), Dy(3)–Mn(2) = 3.3829(10), Dy(1)–Dy(2) = 3.818(5), Dy(3)–Dy(2) = 3.824(5), Mn(1)–O(10)–Dy(1) = 106.55(18), Mn(1)–O(5)–Dy(1) = 101.98(16), Dy(1)–O(6)–Dy(2) = 114.09(16), Dy(1)–O(9)–Dy(2) = 107.61(15), Dy(3)–O(18)–Dy(2) = 113.83(16), Dy(3)–O(13)–Dy(2) = 109.01(16), Mn(2)–O(14)–Dy(3) = 105.07(18), Mn(2)–O(17)–Dy(3) = 100.77(17), Dy(1)–Dy(2)–Dy(3) = 164.97(1), Mn(1)–Dy(1)–Dy(2) = 97.85(2), Mn(2)–Dy(3)–Dy(2) = 93.51(2).

dx.doi.org/10.1021/ic4028833 | *Inorg. Chem.* 2014, 53, 6524–6533

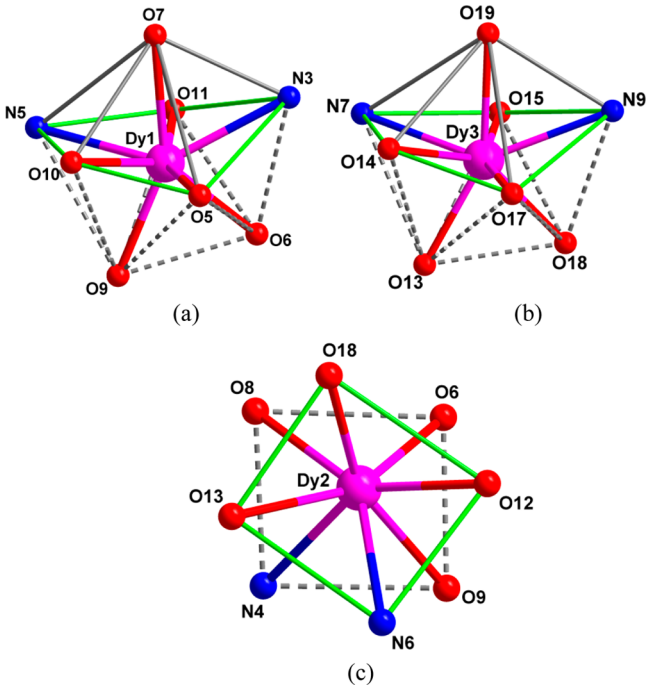

Figure 5. Distorted trigonal dodecahedral geometry around (a) Dy1, (b) Dy3. (c) Distorted square antiprism geometry around Dy2 of the dysprosium(III) ions in **2**. Selected bond distances (Å) are as follows: Dy(1)−O(6) = 2.244(4), Dy(1)−O(9) = 2.310(4), Dy(1)−O(11) = 2.337(4), Dy(1)−O(10) = 2.348(4), Dy(1)−O(7) = 2.410(4), Dy(1)−O(5) = 2.442(4), Dy(1)−N(3) = 2.557(5), Dy(1)−N(5) = 2.586(5), Dy(2)−O(6) = 2.306(4), Dy(2)−O(18) = 2.325(4), Dy(2)−O(8) = 2.331(4), Dy(2)−O(12) = 2.334(4), Dy(2)−O(13) = 2.417(4), Dy(2)−O(9) = 2.421(4), Dy(2)−N(4) = 2.533(5), Dy(2)−N(6) = 2.539(5), Dy(3)−O(18) = 2.238(4), Dy(3)−O(13) = 2.279(4), Dy(3)−O(15) = 2.358(4), Dy(3)−O(14) = 2.370(4), Dy(3)−O(19) =2.401(4), Dy(3)−O(17) = 2.458(4), Dy(3)−N(9) = 2.547(5), Dy(3)−N(7) = 2.595(5).

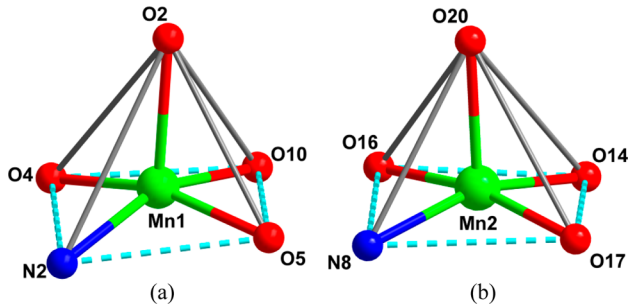

Figure 6. Distorted square pyramidal geometry around (a) Mn1, (b) Mn2. Selected bond distances (Å) are as follows: Mn(1)−O(4) = 1.862(4), Mn(1)−O(10) = 1.875(4), Mn(1)−O(5) = 1.909(4), Mn(1)−N(2) = 1.989(5), Mn(1)−O(2) = 2.126(4), Mn(2)−O(16) = 1.857(4), Mn(2)−O(14) = 1.875(4), Mn(2)−O(17) = 1.910(4), Mn(2)−N(8) = 1.986(5), Mn(2)−O(20) = 2.135(5).

parameters of **2** are summarized in captions of Figures 4−6. The molecular structures and selected bond parameters of the other compounds are given in the Supporting Information (Figures S1−S3, Tables S2−S4).

Detailed structural analysis reveals that the formation of these pentanuclear complexes involves four triply deprotonated $[LH]^{3-}$ ligands. Each of the ligands simultaneously binds three metal ions in a μ_3-η^2:η^1:η^1:η^2:η^1:η^1 fashion and is made possible

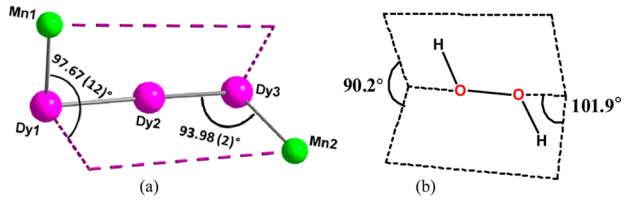

Figure 7. Arrangement of (a) $Mn^{III}_2Dy_3$ unit in open-book type topology in **2** analogous to that found in one of the conformations of hydrogen peroxide (b).

through the deprotonation of one of the ethanolamine arms (CH_2OH) while keeping the other arm intact. We have confirmed this assignment of protonation level on the alkoxy oxygens, as well as the +3 oxidation state of both the manganese ions through BVS calculations (Table 2 and

Table 2. Bond Valence Sum (BVS) Calculations for Assigning the Protonation Level on Oxygen Atoms of the LH^{3-} in Complex 2

Atom	BVS	Assignment
O6	1.991	RO^-
O7	1.187	ROH
O10	1.987	RO^-
O11	1.274	ROH
O14	1.932	RO^-
O15	1.281	ROH
O18	1.967	RO^-
O19	1.243	ROH
O20	1.135	H_3COH

Supporting Information).[22] The BVS value of ∼1.15 suggests that the terminally bound oxygen atoms (O7, O11, O15, O19, and O20) remain in their native form, while the corresponding value of ∼2 for the bridging alcoholic oxygens (O6, O10, O14, and O18) confirms their deprotonated state. It is quite evident from the structure of **2** that the pentanuclear core consists of two terminal $[MnDyO_2]$ and two central $[Dy_2O_2]$ four-membered rings, and notably they are contiguous to each other and both types of rings are composed of one phenolate and one alkoxide oxygen atoms. The most remarkable feature of the molecular structure is that all three Dy(III) ions are arranged in a near-linear fashion with a Dy···Dy···Dy angle of ∼165° and remain at the junction of the two planes constituted by Mn1−Dy1−Dy2−Dy3 and Mn2−Dy3−Dy2−Dy1; the interplanar angle is 97.67(12)° with inter Dy···Dy distances of 3.818(5) (Dy1−Dy2), 3.824(5) (Dy2−Dy3), and 7.576(5) Å (Dy1−Dy3). If one looks at the pentametallic core alone, it has a topology of an open book that is analogous to that found in one of the conformations of hydrogen peroxide (Figure 7). Among the three lanthanide ions, the central lanthanide (Dy2) possesses a different coordination environment from the two terminal ones (Dy1, Dy3). Thus, although all three Dy(III) ions are octacoordinated (6O, 2N), Dy1 and Dy3 possess a $-[CH_2-CH_2-OH]$ ligand in their coordination environment. As a result Dy2 adopts a distorted square-antiprism geometry while Dy1 and Dy3 possess a distorted trigonal-dodecahedral geometry (Figure 5) The two Mn(III) ions are both pentacoordinated (4O, 1N) and possess a distorted square pyramidal geometry (Figure 6). The basal plane consists of two phenolate, one *N*-ethoxide oxygen, and one imino nitrogen

dx.doi.org/10.1021/ic4028833 | Inorg. Chem. 2014, 53, 6524−6533

atoms, while the apical position is occupied by the oxygen atom either from a η^1-nitrate ion (O2) or from a methanol molecule (O20) for Mn1 and Mn2, respectively. The Mn···Dy distances involved are 3.3829(10) and 3.3970(10) Å.

The crystal structure of **2** reveals the formation of both 1D and 2D supramolecular polymeric association through intermolecular C−H···.O noncovalent interactions mediated by both by Mn(1)-bound nitrate ion and the perchlorate counteranion (Supporting Information).

Magnetic Properties. Magnetic susceptibility measurements were carried out on polycrystalline samples under a dc field of 500 Oe, in the temperature range 1.8−300 K. The evolution of the χT product for **1**−**4** is presented in Figure 8.

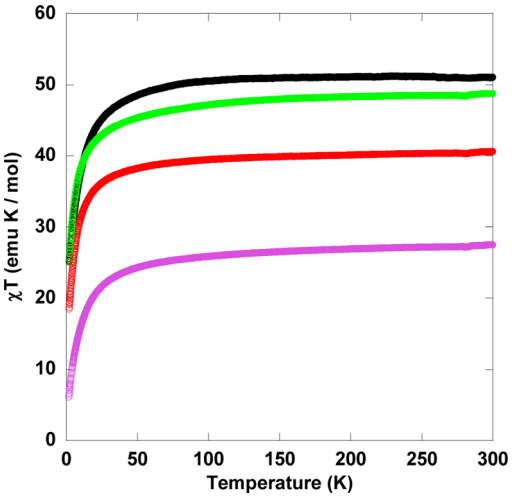

Figure 8. Evolution of the χT product as a function of T for **1** (purple), **2** (black), **3** (red), and **4** (green) under a 500 Oe applied dc field.

The values at room temperature (27.3, 51.02, 40.5, and 48.7 emu·K·mol^{-1} for **1**, **2**, **3**, and **4**, respectively) are in relatively good agreement with the expected ones (29.64, 48.51, 41.46, and 48.21 emu·K·mol^{-1} for **1**, **2**, **3**, and **4**, respectively) for the two Mn(III) (S = 2, g = 2) and three Ln(III) ions (Gd(III): ground state $^8S_{7/2}$, g_J = 2, $\chi T_{\text{free ion}}$ = 7.88 emu·K·mol^{-1}, Dy(III): $^6H_{15/2}$, g_J = 4/3, $\chi T_{\text{free ion}}$ = 14.17 emu·K·mol^{-1}, Tb(III): $^7F_6$, g_J = 3/2, $\chi T_{\text{free ion}}$ = 11.82 emu·K·mol^{-1}, Ho(III): $^5I_8$, g_J = 5/4, $\chi T_{\text{free ion}}$ = 14.07 emu·K·mol^{-1}).[10c]

For all the compounds, the χT product decreases regularly upon cooling. For the Gd(III) analogue, the $\chi T = f(T)$ curve can be fitted considering the following spin Hamiltonian:

$\hat{H} = -J_1 (\hat{S}_{Mn1}\cdot\hat{S}_{Gd1} + \hat{S}_{Mn2}\cdot\hat{S}_{Gd3}) - J_2\hat{S}_{Gd2}\cdot(\hat{S}_{Gd1} + \hat{S}_{Gd3})$

(Figure 9) using the Magpack program.[23] The magnetic anisotropy of the Mn(III) ions, as well as the intermolecular interactions, are thus neglected. The fit leads to g = 1.93(2), J_1 = −0.23(1) cm^{-1}, and J_2 = −0.68(1) cm^{-1}, with a very good agreement factor $R = 2 \times 10^{-5}$. The value of J_1 lies within the range of values usually encountered for 3d-Gd(III) interaction.[24] J_2 appears to be quite large (about one order one magnitude larger) than what is usually found for Gd−Gd interaction.[17] This probable overestimation is likely due to the fact that we have neglected single ion anisotropy of Mn(III). Yet, if we consider this single ion anisotropy, we have to neglect the Gd−Gd interaction; otherwise, the problem is clearly overparametrized. These considerations lead to far poorer fits of $\chi T = f(T)$ and of $M = f(H)$.

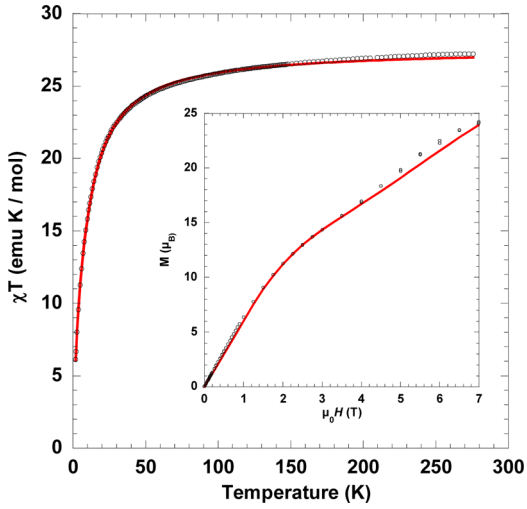

Figure 9. Fit of $\chi T = f(T)$ for compound **1** (open circles: experimental, full line: fit (see text)). Inset: $M = f(H)$ curve for compound **1** (open circles: experimental, full line: calculated curve using the values obtained from the fit of the $\chi T = f(T)$ curve).

Although the approximations made for the fitting of the $\chi T = f(T)$ curve for **1** are rather important (the single ion anisotropy of Mn(III) ions and the intermolecular interactions have been neglected), it is worth noticing that the set of values obtained from the fit allows good reproduction of the magnetization curve, especially the inflection point around 3 T (see below), which tends to validate the approximations made.

For the other compounds, the regular decrease of the χT product suggests intramolecular antiferromagnetic interactions. At very low temperatures, thermal depopulation of low-lying crystal-field states of the Ln(III) ions can also contribute to the decrease of χT[10c] (given the very large distance between the molecules (above 10 Å), intermolecular magnetic interactions are likely negligible with respect to intramolecular ones). It is indeed noticeable from the fit of χT $f(T)$ for **1** that the intermolecular coupling is very small. The intermolecular coupling in the other compounds can be reasonably estimated to be of the same order of magnitude. At low temperature, it is thus comparable to the thermal depopulation effect.

The magnetization vs field curves measured at 1.8 K are reported in Figure 10. There again, the four compounds exhibit slightly different behavior. The derivatives of the curves are reported in Supporting Information.

For **1**, the magnetization increases rather slowly at low fields until an inflection point at 3.4 T. The value of the magnetization at the inflection point (around 15 μ_B) corresponds to the antiparallel alignment of the moment of the central Gd(III) ion (Gd2) with the ones of the other spin carriers. In other words, the field at the inflection point corresponds to the field necessary to counterbalance the antiferromagnetic interaction between the Mn(III) ions and the external Gd(III) ions (Gd1 and Gd3) (the system goes from the antiferromagnetic ground state $\alpha-\beta-\alpha-\beta-\alpha$ to the excited state of configuration $\alpha-\alpha-\beta-\alpha-\alpha$ where α stands for a spin up, and β for a spin down). The field at the inflection point thus provides a qualitative estimation of J_{Mn-Gd}. When the magnetic field becomes larger, the magnetization continues to increase after the inflection point, due to the field-induced reversal of the moment of the central Gd(III) ion. Full alignment of all the spins would correspond to the saturation

dx.doi.org/10.1021/ic4028833 | Inorg. Chem. 2014, 53, 6524−6533

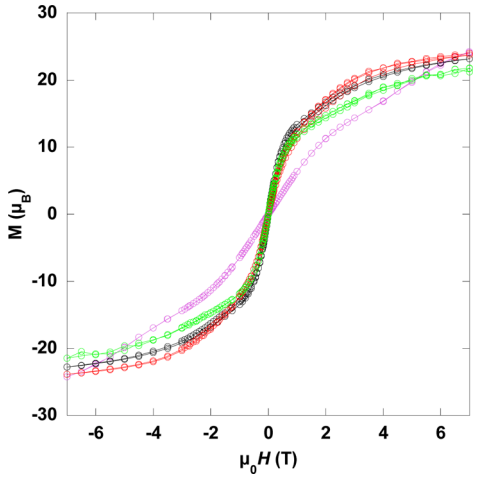

Figure 10. Magnetization vs field curves for **1** (purple), **2** (black), **3** (red), and **4** (green) at 1.8 K (full lines are just guides for the eye).

value, not reached with the experimental fields, of around 29 μ_B. The same situation occurs for **2**, with an inflection point at 1.2 T (14 μ_B), a little bit lower than the expected value for the antiparallel alignment of the moment of Dy2 with the moments of the other ions (about 18 μ_B) ($\alpha-\alpha-\beta-\alpha-\alpha$ spin configuration). This behavior confirms the antiferromagnetic nature of the Mn−Gd and Mn−Dy interactions. It has to be compared to the ones of the Ni_2Gd_3 and Ni_2Dy_3 analogues, for which there was no inflection point on the $M = f(H)$ curves, the Ni(II) ions being diamagnetic.[17] For **3** and **4** no inflection point could be evidenced on the magnetization curve up to 7 T which indicates stronger 3d−4f antiferromagnetic interactions. For compounds **2**−**4**, the high-field values of the magnetization (23.2, 23.8, and 21.5 μ_B for **2**, **3**, **4**, respectively) are in agreement with the expected ones (between 22 and 25 μ_B). Indeed, due to the crystal field effects the values of saturation magnetization for Dy(III), Tb(III), and Ho(III) range between 4.5 μ_B and 6 μ_B.[24a] For **1**, the expected value is higher, around 29 μ_B, because the $^8S_{7/2}$ ground state of Gd(III) is isotropic. The experimental value of the magnetization at high-field, which is clearly not saturated, is much lower than the expected one, probably because of the relatively large Gd−Gd interaction.

AC susceptibility measurements were performed without applied static field in the temperature range 1.8−30 K with a 1 Oe field oscillating at frequencies ranging from 1000 to 1 Hz. For **1** and **3**, all the in-phase susceptibility curves are superimposable down to 1.8 K, and no out-of-phase signal appears, which indicates the absence of slow relaxation of the magnetization. For **2** and **4**, a clear frequency dependent out-of-phase signal appears below 5 K, while the in-phase susceptibility curves are no longer superimposable at low temperature (Supporting Information Figures S12 and S13). This behavior suggests a slow relaxation of the magnetization, corresponding to single-molecule magnet behavior. Yet, the very low temperature at which this behavior occurs, most probably because of quantum tunneling of the magnetization,[25] prevents quantitative determination of the parameters (energy barrier, pre-exponential factor).

In order to overcome this difficulty, ac susceptibility measurements were performed under an optimized small dc field (2000 Oe) (Supporting Information Figure S14). Only **2** showed maxima in the temperature dependence on χ' and χ'' under this dc field (Figure 11). This result is in accordance with the previously reported observation on other lanthanide complexes, according to which only the Kramers systems with odd numbers of electrons show that this dc field induced SMM behavior.[26]

Given the very low temperature at which they occur, it is only possible to extract three maxima from this experiment. Therefore, the nature of the relaxation mechanism cannot be ascertained unambiguously to a thermally activated process. Yet, the three points obtained by plotting the magnetization relaxation times determined from the $\chi'' = f(T)$ curve as $\ln(\tau) = f(T^{-1})$, are aligned. By fitting this "curve" to an Arrhenius law $\tau = \tau_0 \exp(U_{eff}/kT)$, it is possible to extract the activation barrier U_{eff}/k = 13 K, and the pre-exponential factor $\tau_0 = 5 \times 10^{-6}$ s (Supporting Information Figure S15). These parameters are within the range of the values reported for other lanthanide-based SMMs.[26]

The low temperature frequency-dependent ac susceptibility data for compound **2** was further analyzed using a generalized

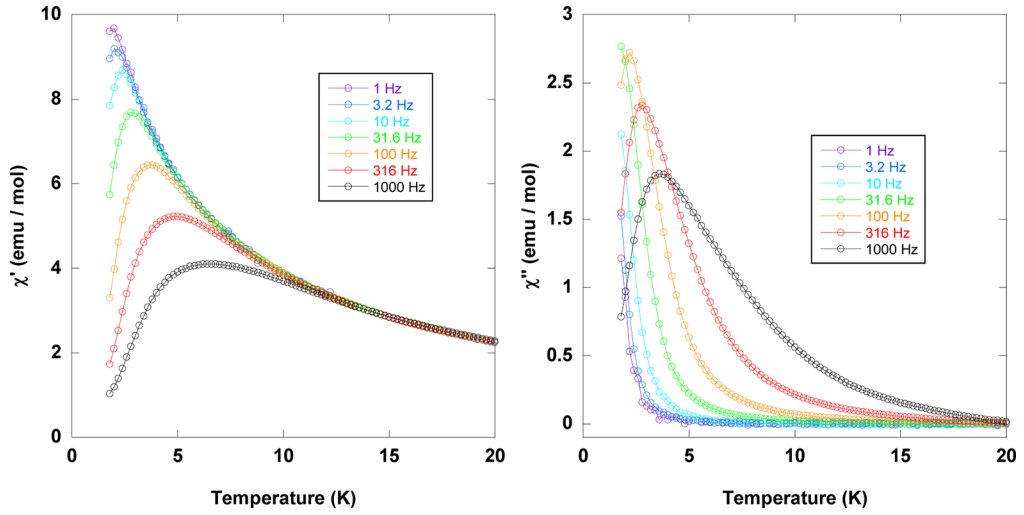

Figure 11. In-phase (left) and out-of-phase (right) susceptibility measurements at various frequencies for compound **2** under an applied dc field of 2000 Oe and with an oscillating field of 2 Oe.

dx.doi.org/10.1021/ic4028833 | Inorg. Chem. 2014, 53, 6524−6533

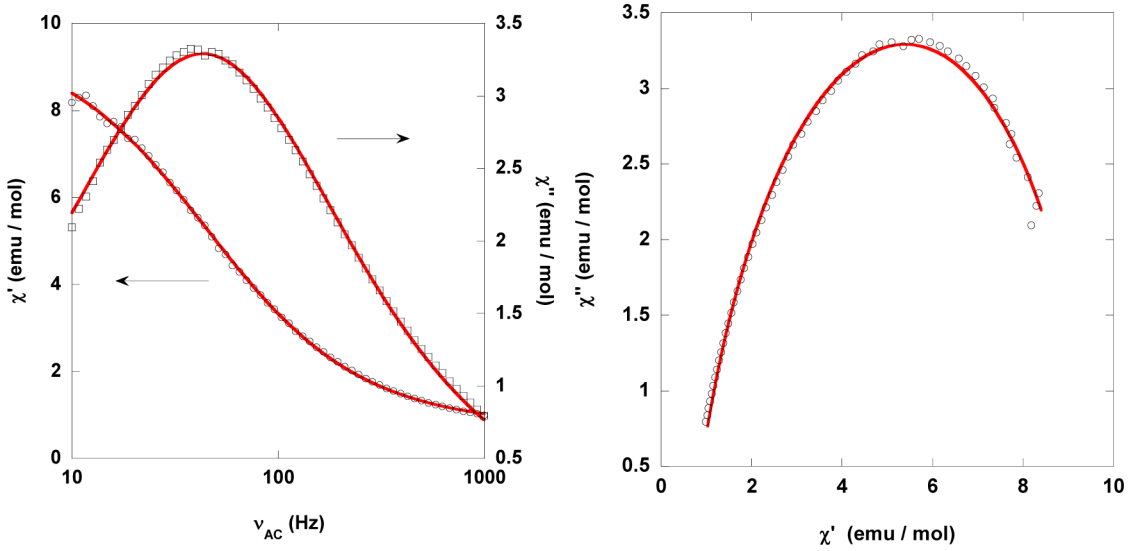

Figure 12. Left: plots of the in-phase susceptibility (open circles) and out-of-phase susceptibility (open circles) for **2** at 1.8 K (applied dc field of 2000 Oe, oscillating field of 2 Oe). Right: Cole−Cole plot. The solid lines correspond to the fit of the data to a generalized Debye model.

Debye model to fit the Cole−Cole plot (see Supporting Information for the fit information) (Figure 12).[27]

The best fit of the Cole−Cole plot at 1.8 K leads to the following parameters: $\alpha = 0.23(1)$, $\chi_0 = 9.95(5)$ emu·mol^{-1}, $\chi_\infty = 0.55(2)$ emu·mol^{-1}, and $\tau = 0.0036(1)$ s. The values of α and τ are consistent with ones usually encountered for other SMMs. The relatively large value for α indicate a broad distribution of relaxation times, suggesting that more than one relaxation process might operate at this temperature.

In this context it is interesting to compare magnetic properties of the analogous Ni_2Ln_3 compounds with the current members (**1**−**4**). In the Ni_2Ln_3 family, Ni_2Dy_3 shows extensive ferromagnetic coupling in χT vs T plot at low temperature with a concomitant presence of multistep relaxation in the temperature dependent out-of-phase ac susceptibility signal. Eventually, this produces two energy barriers (U_{eff}) 85 K and 53.5 K, and the corresponding time scale for relaxations (τ_0) are 5.9×10^{-7} s and 2.3×10^{-8} s at higher and lower temperatures, respectively.[17] In contrast, **2** presents a much smaller energy barrier (13 K). This behavior is presumably due to the noncolinearity of the individual anisotropic axis of three lanthanide as well as Mn^{III} ions. Consequently, the net anisotropy of the whole molecule and hence the energy barrier of the complexes (**2**, **4**) for spin flip become less, and also weak spin−spin interactions among the Mn(III) and Ln(III) ions play a crucial role in fast magnetization relaxation in **2** and **4**. Also, in the Ni/Ln complexes both the Ni(II) ions are diamagnetic, and therefore magnetic contributions arise exclusively from the highly anisotropic Dy(III) ions. Similar "negative influence" of the single ion anisotropy has been recently studied in Co-Ln-Co SMMs, for which it has been shown that the most efficient magnetic blockage was obtained for the isotropic Gd, whereas anisotropic Tb and Dy lead to less efficient blockage.[28] The presence of low-lying excited spin states, due to the very small magnetic interactions, may also be responsible for the small effective barrier.

CONCLUSION

In summary, we have successfully isolated a new family of pentanuclear, dicationic, heterometallic $\{Mn^{III}_2Ln^{III}_3\}$ complexes with an open-book type structural topology. This was made possible by use of an unsymmetrically substituted multisite coordinating Schiff base ligand (LH_4). Overall four trianionic ligands are involved in holding the pentameric unit. In this pentameric unit, both manganese ions are placed in the periphery and are pentacoordinated having a square pyramidal geometry. On the other hand, three lanthanide(III) ions remain at the center almost in a linear fashion and are octacoordinated. The geometry around the peripheral lanthanides is trigonal-dodecahedron while a square-antiprism geometry was found for the central lanthanide (III) ion. Magnetochemical analysis reveals the presence of overall antiferromagnetic interactions among the spin centers at low temperatures in all the four compounds. The ac susceptibility measurements reveal that among the four compounds (**1**−**4**) only **2** and **4** show frequency-dependent out-of-phase ac signals without a maxima in zero applied dc field in spite of the presence of Mn(III) ion in all of them. For **2** it has been possible to extract the relaxation parameters by applying a 2000 Oe dc field. Therefore, it can be concluded that the manifestation of SMM behavior in the compounds **2** and **4** arises presumably from the Ln(III) ions or from a combination of both Ln(III) and Mn(III) ions. In line with the systematic study here, we are trying to develop other 3d/4f complexes by specific replacement of 3d ions using the same ligand (LH_4) in order to get an overall idea about the magnetic interactions among the 3d metal ions with Ln(III) ions in these type of complexes. Such studies are in progress in our laboratory.

ASSOCIATED CONTENT

Supporting Information

CIF file and BVS values, bond distances and angles, structures, ESI-MS spectra, and Cole-Cole plot fits. This material is available free of charge via the Internet at http://pubs.acs.org.

AUTHOR INFORMATION

Corresponding Authors

*E-mail: vc@iitk.ac.in.
*E-mail: Guillaume.Rogez@ipcms.unistra.fr.

dx.doi.org/10.1021/ic4028833 | Inorg. Chem. 2014, 53, 6524−6533

Notes

The authors declare no competing financial interest.

■ ACKNOWLEDGMENTS

V.C. is thankful to the Department of Science and Technology, India for a J. C. Bose fellowship. P. B. and A. C. thank Council of Scientific and Industrial Research, India, for Senior Research Fellowship.The authors thank Dr. E. Rivière, ICMMO, University of Paris Sud Orsay for his help with the MagPack software. Finally the authors thank the referees for their very valuable remarks and suggestions.

■ REFERENCES

(1) Sessoli, R.; Tsai, H.-L.; Schake, A. R.; Wang, S.; Vincent, J. B.; Folting, K.; Gatteschi, D.; Christou, G.; Hendrickson, D. N. *J. Am. Chem. Soc.* **1993**, *115*, 1804.

(2) (a) Miller, J. S.; Drillon, M. *Magnetism: Molecules to Materials III*; Wiley-VCH: Weinheim, 2002. (b) Christou, G.; Gatteschi, D.; Hendrickson, D. N.; Sessoli, R. *MRS Bull.* **2000**, *25*, 66. (c) Ritter, S. K. *Chem. Eng. News* **2004**, *82*, 29.

(3) (a) Thomas, L.; Lionti, F.; Balou, R.; Gatteschi, D.; Sessoli, R.; Barbara, B. *Nature* **1996**, *383*, 145. (b) Rinehart, J. D.; Fang, M.; Evans, W. J.; Long, J. R. *Nat. Chem.* **2011**, *3*, 538. (c) Mannini, M.; Pineider, F.; Sainctavit, P.; Danieli, C.; Otero, E.; Sciancalepore, C.; Talarico, M. A.; Arrio, M.-A.; Cornia, A.; Gatteschi, D.; Sessoli, R. *Nat. Mater.* **2009**, *8*, 194. (d) Lin, P. H.; Burchell, T. J.; Clérac, R.; Murugesu, M. *Angew. Chem., Int. Ed.* **2008**, *47*, 8848. (e) Sessoli, R.; Gatteschi, D.; Caneschi, A.; Novak, M. A. *Nature* **1993**, *365*, 141.

(4) (a) Wernsdorfer, W.; Sessoli, R. *Science* **1999**, *284*, 133. (b) Gatteschi, D.; Sessoli, R. *Angew. Chem., Int. Ed.* **2003**, *43*, 268. (c) Hill, S.; Edward, R. S.; Aliaga-Alcalde, N.; Christou, G. *Science* **2003**, *302*, 1015. (d) Friedman, J. R.; Sarachik, M. P.; Tejada, J.; Ziolo, R. *Phys. Rev. Lett.* **1996**, *76*, 3830.

(5) (a) Tang, J.; Hewitt, I.; Madhu, N. T.; Chastanet, G.; Wernsdorfer, W.; Anson, C. E.; Benelli, C.; Sessoli, R.; Powell, A. K. *Angew. Chem., Int. Ed.* **2006**, *45*, 1729. (b) Kahn, O. *Acc. Chem. Res.* **2000**, *33*, 647. (c) Murrie, M. *Chem. Soc. Rev.* **2010**, *39*, 1986. (d) Sessoli, R.; Powell, A. K. *Coord. Chem. Rev.* **2009**, *253*, 2328.

(6) (a) Ardavan, A.; Rival, O.; Morton, J. J. L.; Blundell, S. J.; Tytyshkin, A. M.; Timco, G. A.; Winpenny, R. E. P. *Phys. Rev. Lett.* **2007**, *98*, 057201. (b) Candini, A.; Klyatskaya, S.; Ruben, M.; Wernsdorfer, W.; Affronte, M. *Nano Lett* **2011**, *11*, 2634. (c) Tejada, J.; Chudnovsky, E. M.; del Barco, E.; Hernandez, J. M.; Spiller, T. P. *Nanotechnology* **2001**, *12*, 181.

(7) (a) Leuenberger, M. N.; Loss, D. *Nature* **2001**, *410*, 789. (b) Stamp, P. C. E.; Gaita-Ariño, A. *J. Mater. Chem.* **2009**, *19*, 1718. (c) Winpenny, R. E. P. *Angew. Chem., Int. Ed.* **2008**, *47*, 7992.

(8) (a) Evangelisti, M.; Roubeau, O.; Palacios, E.; Camón, A.; Hooper, T. N.; Brechin, E. K.; Alonso, J. J. *Angew. Chem., Int. Ed.* **2011**, *50*, 6606. (b) Sharples, J. W.; Zheng, Y.-Z.; Tuna, F.; McInnes, E. J. L.; Collison, D. *Chem. Commun.* **2011**, *47*, 7650. (c) Evangelisti, M.; Luis, F.; de Jongh, L. J.; Affronte, M. *J. Mater. Chem.* **2006**, *16*, 2534. (d) Shi, P.-F.; Zheng, Y.-Z.; Zhao, X.-Q.; Xiong, G.; Zhao, B.; Wan, F.-F.; Cheng, P. *Chem.—Eur. J.* **2012**, *18*, 15086. (e) Sessoli, R. *Angew. Chem., Int. Ed.* **2012**, *51*, 43. (f) Zheng, Y.-Z.; Evangelisti, M.; Tuna, F.; Winpenny, R. E. P. *J. Am. Chem. Soc.* **2012**, *134*, 1057.

(9) (a) Murugesu, M. *Nat. Chem.* **2012**, *4*, 347. (b) Oshio, H.; Nakano, M. *Chem.—Eur. J.* **2005**, *11*, 5178. (c) Cirera, J.; Ruiz, E.; Alvarez, S.; Neese, F.; Kortus, J. *Chem.—Eur. J.* **2009**, *15*, 4078. (d) Nakano, M.; Oshio, H. *Chem. Soc. Rev.* **2011**, *40*, 3239.

(10) (a) Wanga, S.; Dinga, X.-H.; Lia, Y.-H.; Huang, W. *Coord. Chem. Rev.* **2012**, *256*, 439. (b) Tasiopoulos, A. J.; Vinslava, A.; Wernsdorfer, W.; Abboud, K. A.; Christou, G. *Angew. Chem., Int. Ed.* **2004**, *43*, 2117. (c) Benelli, C.; Gatteschi, D. *Chem. Rev.* **2002**, *102*, 2369.

(11) (a) Sorace, L.; Benelli, C.; Gatteschi, D. *Chem. Soc. Rev.* **2011**, *40*, 3092. (b) Woodruff, D. N.; Winpenny, R. E. P.; Layfield, R. A. *Chem. Rev.* **2013**, *113*, 5110. (c) Zhang, P.; Guo, Y.-N.; Tang, J. *Coord. Chem. Rev.* **2013**, *257*, 1728.

(12) (a) Andruh, M.; Costes, J.-P.; Diaz, C.; Gao, S. *Inorg. Chem.* **2009**, *48*, 3342. (b) Mondal, K. C.; Sundt, A.; Lan, Y.; Kostakis, G. E.; Waldmann, O.; Ungur, L.; Chibotaru, L. F.; Anson, C. E.; Powell, A. K. *Angew. Chem., Int. Ed.* **2012**, *51*, 7550. (c) Winpenny, R. E. P. *Chem. Soc. Rev.* **1998**, *27*, 447. (d) Schray, D.; Abbas, G.; Lan, Y.; Mereacre, V.; Sundt, A.; Dreiser, J.; Waldmann, O.; Kostakis, G. E.; Anson, C. E.; Powell, A. K. *Angew. Chem., Int. Ed.* **2010**, *49*, 5185. (e) Chandrasekhar, V.; Pandian, B. M.; Vittal, J. J.; Clérac, R. *Inorg. Chem.* **2009**, *48*, 1148.

(13) (a) Osa, S.; Kido, T.; Matsumoto, N.; Re, N.; Pochaba, A.; Mrozinski, J. *J. Am. Chem. Soc.* **2004**, *126*, 420. (b) Novitchi, G.; Wernsdorfer, W.; Chibotaru, L. F.; Costes, J. P.; Anson, C. E.; Powell, A. K. *Angew. Chem., Int. Ed.* **2009**, *48*, 1614. (c) Feltham, H. L. C.; Clérac, R.; Powell, A. K.; Brooker, S. *Inorg. Chem.* **2011**, *50*, 4232. (d) Baskar, V.; Gopal, K.; Helliwell, M.; Tuna, F.; Wernsdorfer, W.; Winpenny, R. E. P. *Dalton Trans.* **2010**, *39*, 4747. (e) Chandrasekhar, V.; Dey, A.; Das, S.; Rouzières, M.; Clérac, R. *Inorg. Chem.* **2013**, *52*, 2588. (f) Novitchi, G.; Pilet, G.; Ungur, L.; Moshchalkov, V. V.; Wernsdorfer, W.; Chibotaru, L. F.; Luneau, D.; Powell, A. K. *Chem. Sci.* **2012**, *3*, 1169. (g) Feltham, H. L. C.; Clérac, R.; Ungur, L.; Chibotaru, L. F.; Powell, A. K.; Brooker, S. *Inorg. Chem.* **2013**, *52*, 3236.

(14) (a) Mereacre, V. M.; Ako, A. M.; Clérac, R.; Wernsdorfer, W.; Filoti, G.; Bartolome, J.; Anson, C. E.; Powell, A. K. *J. Am. Chem. Soc.* **2007**, *129*, 9248. (b) Saha, A.; Thompson, M.; Abboud, K. A.; Wernsdorfer, W.; Christou, G. *Inorg. Chem.* **2011**, *50*, 10476. (c) Mereacre, V.; Ako, A. M.; Clérac, R.; Wernsdorfer, W.; Hewitt, I. J.; Anson, C. E.; Powell, A. K. *Chem.—Eur. J.* **2008**, *14*, 3577. (d) Zaleski, C. M.; Depperman, E. C.; Kampf, J. W.; Kirk, M. L.; Pecoraro, V. L. *Angew. Chem., Int. Ed.* **2004**, *43*, 3912. (e) Liu, J.-L.; Guo, F.-S.; Meng, Z.-S.; Zheng, Y.-Z.; Leng, J.-D.; Tong, M.-L.; Ungur, L.; Chibotaru, L. F.; Heroux, K. J.; Hendrickson, D. N. *Chem. Sci.* **2011**, *2*, 1268. (f) Mishra, A.; Wernsdorfer, W.; Abboud, K. A.; Christou, G. *J. Am. Chem. Soc.* **2004**, *126*, 15648. (g) Holynska, M.; Premuzic, D.; Jeon, I.-R.; Wernsdorfer, W.; Clerac, R.; Dehnen, S. *Chem.—Eur. J.* **2011**, *17*, 9605. (h) Ke, H.; Zhao, L.; Guoa, Y.; Tang, J. *Dalton Trans.* **2012**, *41*, 2314. (i) Mereacre, V.; Lan, Y.; Clérac, R.; Ako, A. M.; Hewitt, I. J.; Wernsdorfer, W.; Buth, G.; Anson, C. E.; Powell, A. K. *Inorg. Chem.* **2010**, *49*, 5293. (j) Mishra, A.; Wernsdorfer, W.; Parson, S.; Christou, G.; Brechin, E. *Chem. Commun.* **2005**, 2086.

(15) (a) Akhtar, M. N.; Lan, Y.; Mereacre, V.; Clerac, R.; Anson, C. E.; Powell, A. K. *Polyhedron* **2009**, *28*, 1698. (b) Chandrasekhar, V.; Pandian, B. M.; Boomishankar, R.; Steiner, A.; Clérac, R. *Dalton Trans.* **2008**, 5143. (c) Papatriantafyllopoulou, C.; Wernsdorfer, W.; Abboud, K. A.; Christou, G. *Inorg. Chem.* **2011**, *50*, 421. (d) Chilton, N. F.; Langley, S. K.; Moubaraki, B.; Murray, K. S. *Chem. Commun.* **2010**, *46*, 7787.

(16) Chandrasekhar, V.; Bag, P.; Speldrich, M.; Leusen, J. v.; Kögerler, P. *Inorg. Chem.* **2013**, *52*, 5035.

(17) Chandrasekhar, V.; Bag, P.; Kroener, W.; Gieb, K.; Muller, P. *Inorg. Chem.* **2013**, *52*, 13078.

(18) Furniss, B. S.; Hannaford, A. J.; Smith, P. W. G.; Tatchell, A. R. *Vogel's Text book of Practical Organic Chemistry*, 5th ed.; ELBS; Longman: London,1989.

(19) (a) *SMART & SAINT Software Reference manuals*, version 6.45; Bruker Analytical X-ray Systems, Inc.: Madison, WI, 2003. (b) Sheldrick, G. M. *SADABS, a software for empirical absorption correction*, version 2.05; University of Göttingen, Göttingen, Germany, 2002. (c) *SHELXTL Reference Manual*, version 6.1; Bruker Analytical X-ray Systems, Inc.: Madison, WI, 2000. (d) Sheldrick, G. M. *SHELXT*, version 6.12; BrukerAXS Inc., Madison, WI, 2001. (e) Sheldrick, G. M. *SHELXL97, Program for Crystal Structure Refinement*; University of Göttingen, Göttingen, Germany, 1997. (f) Brandenburg, K. *Diamond*, v 3.1e; Crystal Impact GbR, Bonn, Germany, 2005.

(20) (a) Schmidt, S.; Prodius, D.; Novitchi, G.; Mereacre, V.; Kostakis, G. E.; Powell, A. K. *Chem. Commun.* **2012**, *48*, 9825. (b) Li, M.; Lan, Y.; Ako, A. M.; Wernsdorfer, W.; Anson, C. E.; Buth, G.; Powell, A. K.; Wang, Z.; Gao, S. *Inorg. Chem.* **2010**, *49*, 11587.

(21) Akhtar, M. N.; Zheng, Y.-Z.; Lan, Y.; Mereacre, V.; Anson, C. E.; Powell, A. K. *Inorg. Chem.* **2009**, *48*, 3502.
(22) (a) Liu, W.; Thorp, H. H. *Inorg. Chem.* **1993**, *32*, 4102. (b) Brown, I. D.; Wu, K. K. *Acta Crystallogr.* **1976**, *B32*, 1957.
(23) Borrás-Almenar, J. J.; Clemente-Juan, J. M.; Coronado, E.; Tsukerblat, B. S. *J. Comput. Chem.* **2001**, *22*, 985.
(24) (a) Cremades, E.; Gómez-Coca, S.; Aravena, D.; Alvarez, S.; Ruiz, E. *J. Am. Chem. Soc.* **2012**, *134*, 10532. (b) Rajaraman, G.; Totti, F.; Bencini, A.; Caneschi, A.; Sessoli, R.; Gatteschi, D. *Dalton Trans.* **2009**, 3153.
(25) (a) Campbell, V. E.; Guillot, R.; Rivière, E.; Brun, P.-T.; Werndorfer, W.; Mallah, T. *Inorg. Chem.* **2013**, *52*, 5194−5200. (b) Sugita, M.; Ishikawa, N.; Ishikawa, T.; Koshihara, S.-Y.; Kaizu, Y. *Inorg. Chem.* **2006**, *45*, 1299.
(26) Baniodeh, A.; Lan, Y.; Novitchi, G.; Mereacre, V.; Sukhanov, A.; Ferbinteanu, M.; Voronkova, V.; Anson, C. E.; Powell, A. K. *Dalton Trans.* **2013**, *42*, 8926.
(27) Cole, K. S.; Cole, R. H. *J. Chem. Phys.* **1941**, *9*, 341.
(28) Ungur, L.; Thewissen, M.; Costes, J.-P.; Wernsdorfer, W.; Chibotaru, L. F. *Inorg. Chem.* **2013**, *52*, 6328.

dx.doi.org/10.1021/ic4028833 | *Inorg. Chem.* 2014, 53, 6524−6533